IUBAT Review—A Multidisciplinary Academic Journal, 7(1): 186-201
https://doi.org/10.3329/iubatr.v7i1.74364

Tensile and Fracture Behaviour of Sn/Pb Solder Affected Aluminium Subjected to Post-Deformation Ageing

Mohammad Salim Kaiser[1*]

[1]*Innovation Centre, International University of Business Agriculture and Technology, Dhaka-1230, Bangladesh, ORCID: https://orcid.org/0000-0002-3796-2209*

Keywords:
Aluminium; Sn-Pb solder; Work hardening; Ageing; Tensile strength; Fracture.

Abstract
An efficient assessment of the mechanical characteristics of waste/scraped aluminum under a variety of operating circumstances is crucial to the exploration of its potential for reuse. In this regard Sn/Pb solder affected aluminum is subjected to post-deformation and ageing in order to investigate its effect on tensile and fracture behaviour. To isolate the individual effects pure Al, binary Al-Sn and Al-Pb alloy samples are taken simultaneously. Cold rolled by 80% and aged at different temperatures are then tensile tested at room temperature with a different strain rate. Results are the solder affected samples improved in strength through solid solution strengthening whereas tin performed better than lead because Sn has a different BCC crystal structure than that of FCC Al and Pb. Quantitative analysis indicates that at the peak aged condition the strength of pure aluminium is improved by 21%, 9% and 29% when affected by Sn, Pb and Sn-Pb solder respectively. Tin forms various intermetallics with different impurities hence there is some ageing response. These precipitates have an effect on the strain rate and accelerate the tensile strength. The effects of elements on the reduction of impact strength are noticeable. Minor added alloys show relatively dense grain boundaries for the presence of different elements. Such elements are visible on the fracture surface, which inhibits dislocation movement and ensures high strength.

1. Introduction

The most well-known of the common good-conductive materials are silver, copper, gold, and aluminum (Tehrani, 2021; Woodcraft, 2005). Aluminum is now used for wiring in homes, buildings, aircraft, and appliances due to its greater conductivity to weight ratio and its cost as well as weight benefits over copper. For high-voltage overhead power lines that transport power over great distances, weight is one of the most crucial factors (Davis, 2001). The weight of electrical and electronic

*Corresponding author's E-mail address: dkaiser.res@iubat.edu

Article received: April 29, 2024 Revised and accepted: June 10, 2024 Published: June 30, 2024

components is increasing due to additional functions such as safety and comfort in all types of vehicles. Thus, there is a constant need for aluminum due to both technological advancement and economic growth. Because of this, not enough Al can be extracted from ores to meet requirements; consequently, as natural resources of Al ores are being depleted, there is an increasing reliance on waste/scraped Al-based products. Aluminum bonding is used to join together for structural or thermal purposes. Typically, soldering is used to hold together softer metals, like aluminum. In the areas of electronics, sensors, and electrical power where aluminum contact is required, there aluminum soldering is used. Additionally, it has been employed to seal or repair different types of aluminum heat exchangers (Guan *et al*., 2023). Due to availability, aluminum and its alloys are the most prevalent and have applications in several fields such as transportation, building materials, consumer goods, electrical conductors, and chemical equipment, which is briefly covered in the ASM Handbook (1990).

Aluminum recycling is an outstanding method for secondary material resources (Paraskevas *et al*., 2019). During this process there is a tendency for foreign material to accumulate in the recycled material. That is why it is very important to identify the elements that are present in it for further uses (Kaiser, 2021). It is well established that most of the alloying elements control the various properties of alloys. Sivasankaran, (2017) reported that its quantity can also be a factor in this property. When an element is added it obviously improves one property while affecting other properties. Alloying elements are put in to pure aluminium to strengthen it and occurs through soluble solution strengthening. An additional method is heat treatment to increase Al-alloy's strength. Plastic deformation of materials is an additional method of increasing strength when alloys do not react with heat treatment (Davis, 2001; Kaiser, 2015; Stamenkovic *et al*., 2019).

Furthermore, it is necessary to determine a number of the scraped aluminum's characteristics in order to properly investigate and appropriately identify its engineering applications for the best possible use in the advancement of civilization. In light of this, it is crucial to effectively and thoroughly characterize the various functional properties of waste aluminum in order to maximize the potential of reusing aluminum scrap for new product development. However, research on the possibility of reusing old aluminum wires and components affected by Sn-Pb solder is still lacking. Overall, the effects of this solder on aluminum need to be quantitatively investigated, especially when work hardening with heat treatment. Since the material's mechanical properties are key factors in any used item, the present study examines how solder affects the tensile and fracture behavior of highly plastically deformed aluminum under various thermal treatments. To compare and isolate the individual element effect either Al, Al-Sn and Al-Pb alloys are also considered. This research can significantly facilitate various final products of Al-based alloys with negligible contamination, low energy consumption, high recovery and ease of fabrication.

2. Materials and Methods

Old and waste-soldered connection structures as well as aluminum electrical cables were collected from various sources, melted in an electrical resistance furnace and was cast through a mild steel metal mold conventionally. The cast's chemical composition was then analyzed and showed minor percentages of 1.43 wt% tin and 1.20 wt% lead with Al. Based on this chemical composition three more samples i.e. commercially pure Al, binary Al-Sn and Al-Pb were selected to find out the effect of individual components of solder. Cast samples were put to homogenizing at 450°C, solutionizing at 530°C for 12 h and 2 h respectively and then rapid quenching in water. The schematic diagram of the heat treatment processes of the experimental samples is presented in the following Figure 1.

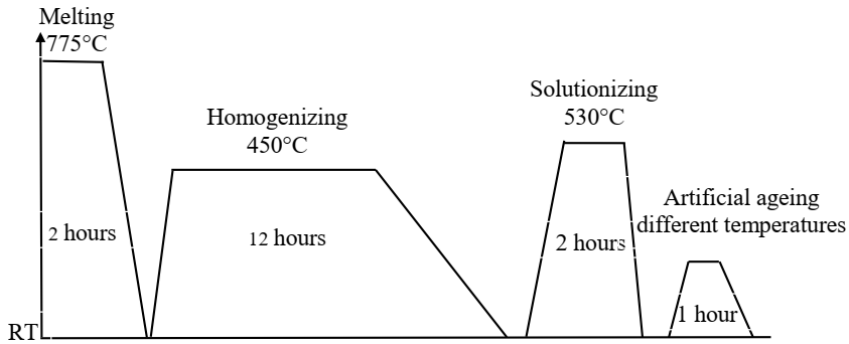

Figure 1: Schematic diagram of the heat treatment processes of the experimental samples.

Emission Spectroscopy was used to examine the casts' chemical compositions, as shown in Table 1. A rolling mill, 10 HP capacity was used at room temperature to deform by 80% of solutionized alloys. Specimen sizes for this cold rolling operation were machined to 15 x 16 x 300 mm to obtain a final thickness of 3 mm after cold rolling. For impact test case size 50 x 25 x 100 mm was considered to get 10 mm thick specimen. Cold rolled samples were given isochronal annealing treatment for one hour at different temperatures. Tensile testing was performed using the standard samples in an 4204 model Instron testing machine of at various strain rates like 10^{-1}/s, 10^{-2}/s, 10^{-3}/s and 10^{-4}/s. The tensile test samples were with a dimension of 25 mm gauge length, 6 mm width, and 3 mm thickness. Again, for the impact test, sample of 10 x 10 x 55 mm with a 2 mm-deep V-shaped notch at a 45° angle was used. Both tests were performed at room temperature according to ASTM guidelines where averages of five test results were considered.

The surfaces of the samples were polished with metallographic sand paper first, in addition to being polished finally with alumina, and the etchant used was Keller's reagent. The reagent consisted of as usual 1volume part of hydrofluoric acid, 1.5 volume part of hydrochloric acid, 2.5 volume parts of nitric acid, and 95 volume parts of distilled water. The etching time was considered around 15 seconds and then

examined the microstructures using a trinocular inverted metal microscope model SKU: ME1200TB-10MA. The tensile fractured samples were subjected to fractographic observations using a JEOL JSM-7600F Scanning Electron Microscope.

Table 1: Compositions of tested samples by weight percentage

Alloy	Sn	Pb	Fe	Si	Cu	Mg	Mn	Ni	Zn	Cr	Ti	Al
Pure Al	0.002	0.002	0.202	0.280	0.008	0.014	0.048	0.008	0.036	0.001	0.002	Bal
Al-Sn	1.512	0.012	0.314	0.335	0.071	0.057	0.106	0.022	0.080	0.002	0.021	Bal
Al-Pb	0.002	1.275	0.335	0.345	0.069	0.055	0.111	0.010	0.075	0.003	0.021	Bal
Al-Sn-Pb	1.433	1.201	0.406	0.435	0.080	0.066	0.108	0.012	0.173	0.020	0.028	Bal

3. Results and Discussion

3.1 Tensile properties

Figure 2 displays the response of the ultimate tensile strength, tested at a strain rate of 10^{-3}s of 80% cold-rolled commercially pure Al, binary Al-Sn, Al-Pb and solder-affected Al-Sn-Pb alloys. All the cases isochronally aging is considered for a period of one hour. The solder affected alloy initially shows the highest strength followed by dopant Sn, Pb and then commercially pure Al. These scenarios can be explained very simply as solid solution strengthening. More specifically, the size of Pb atoms and Sn atoms is larger than that of Al, thus creating a local stress field resulting in higher strength. Although the atomic size of Sn is smaller compare to Pb but shows high strength due to its BCC crystal structure which is different from Al crystal structure like same FCC structure of Pb (Bhat *et al*., 2021).

When aged at 100°C, alloys gain some strength where pure Al and Al-Pb exhibit the insignificant effects. All the alloys contain a trace amount of external elements such as Fe, Si, Mg, Ni, Cu, Ti etc. which come from the melting environment of furnaces linings, ladles, reactors, etc. as specified in Table 1. The formation of GP zones along with the metastable phase during aging can be attributed to this phenomenon. The phase diagram of Al-Sn and Al-Pb demonstrate that with Al no intermetallic formation occurs between them during heat treatment (McAlister,1984; McAlister & Kahan, 1983). But various intermetallics may be formed with Sn but Pb does not. Hence, there is a symptom of ageing for Sn addition rather than Pb. The solder affected alloy obviously shows the highest strength for both Sn and Pb elements effect. The fine precipitates act as a barrier to the dislocation movement, resulting in increased tensile strength. It may be noted that a softening is observed at an early stage for all the alloys due to stress relieving as well as dissolution of GP zones (Ard *et al.*, 2015; Nagy *et al*., 2015).

At higher ageing treatment beyond 250°C, all the alloys drastically fall their strength. It is fully due to over ageing effect. The plastic deformed alloy normally consists of huge dislocation which plays an important role on higher strength. High temperature ageing may be associated with stress relieving, dislocations rearrangement, recovery, precipitation coarsening, recrystallization and grain growth of the alloys (Kaiser, 2020a). When dispersed fine precipitates move into coarse precipitates, reduce the pinning effect and dislocation movements occur more easily as a result lower tensile strength.

The effect of ageing temperature on the yield strength of pure aluminum is shown in Figure 3, and the findings are consistent with the positive impact of solid solution strengthening on the alloys' yield strength. When the ageing treatment of

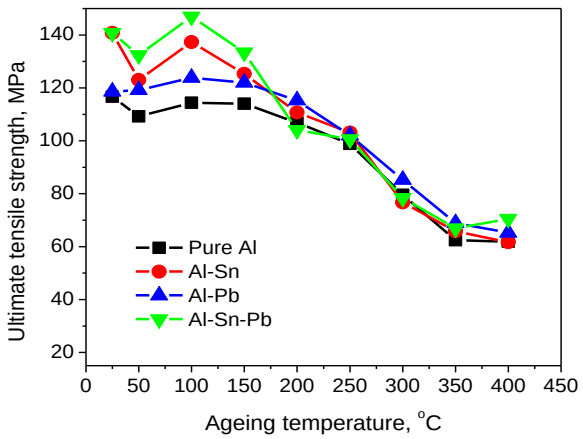

Figure 2: Variations in the ultimate tensile strength of pure Al, binary Al-Sn, Al-Pb, and solder-affected ternary Al-Sn-Pb alloys with isochronally aged for an hour and tensile tested at a strain rate of 10^{-3}/s.

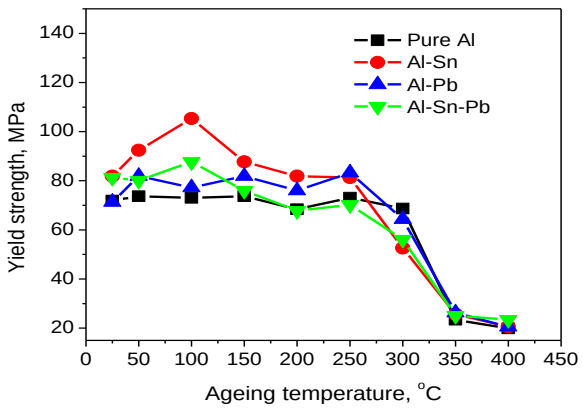

Figure 3: Change of yield strength of the identical experimental samples.

alloys is performed at a lower temperature, just above room temperature like 50°C, the amount of trace precipitates formed inside the microstructure is incredibly tiny. This explains the slight variation in yield strength after this temperature-controlled aging. Ageing at 100°C, the maximum volume fractions of the precipitates are formed into alloys, resulting in a higher influence on the yield strength. The effectiveness is more prominent on the Sn added alloys as already stated regarding the precipitates formation with impurities. There is no noticeable difference of yield strength at high aging temperatures due to the small levels of alloying elements into the alloys.

Again, it may be noticed from the Figure 4, the percentages of elongation decrease with initial ageing temperature and then increases slightly following a drastically increasing beyond the ageing temperature of 250°C. The fact that ductility is minimal in the peak aging condition because of fine precipitates acting as an valuable barrier for dislocation movement. The blocked dislocations resist to plastic deformation resulting lowering elongation (Prabhu, 2017). The content of Sn-added alloys means a higher volume fraction of precipitates and lower ductility. This can be the cause of the lowest ductility of the solder-affected alloy. The observation of improved ductility first due to stress reliving and then precipitate coarsening at higher aging temperatures is in contrast to previous observations for Al-alloys (Kaiser, 2015; Xu *et al.*, 2017).

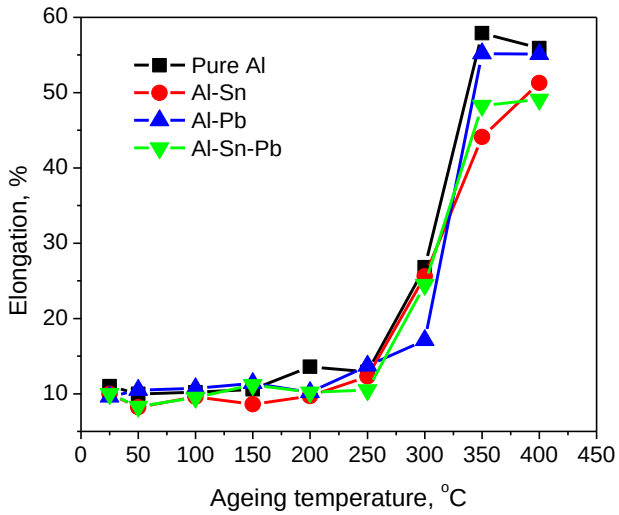

Figure 4: Change of percent elongation of the identical experimental samples.

In Figure 5, the average stress strain ratio to Young's modulus of four experimental samples like Al, Al-Sn, Al-Pb and solder-affected Al-Sn-Pb alloys are plotted against the aging temperature. The values are obviously lower in the under-aged condition and higher in the peak-aged condition. It is due to higher strength and a lower percentage of elongation at peak aged condition. On the contrary, at

high aging temperatures the strength of alloys is very low and the elongation is very high so the ratio is much lower than in the over aged condition. High ageing temperatures cause the dislocations rearrangement and precipitates coarsening which is less effective than fine ones to inhibit dislocation movement (Shoummo *et al.*, 2022). Similar results were obtained for other Al-alloys investigated by Rokon *et al.*, (2023). In all cases solder affected alloys and Sn containing alloys exhibit higher values as expected for their higher strength and lower elongation than the other two alloys.

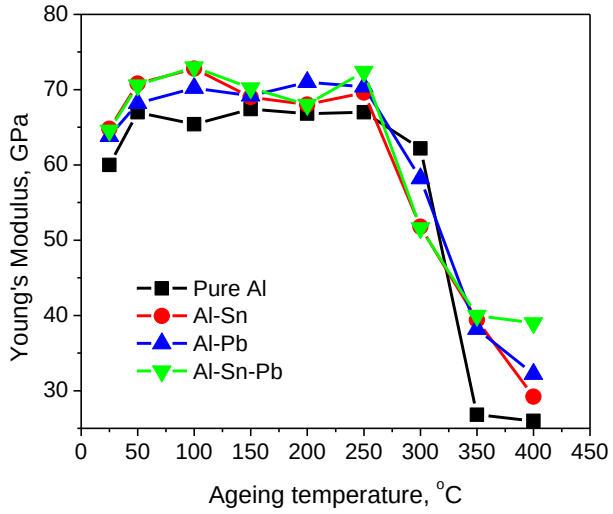

Figure 5: Variation of Young's modulus of the identical experimental samples.

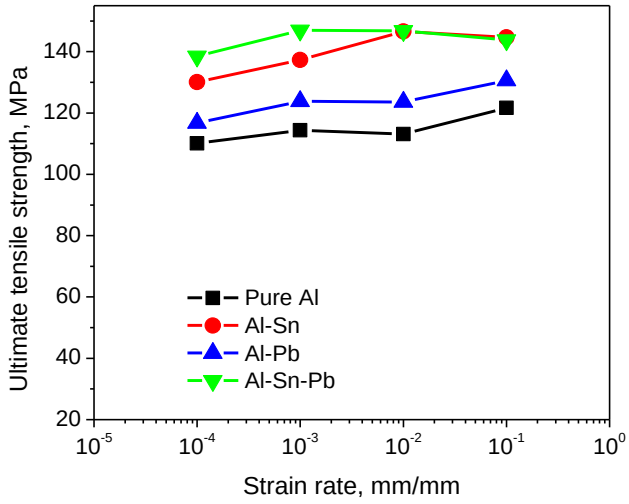

Figure 6: Ultimate ensile strength of cold-rolled alloys aged at 100°C varies with strain. rate.

The variation of ultimate tensile strength, yield strength, percentages of elongation as well as Young's modulus of experimental alloys with strain rates are plotted in the Figures 6 to 9 respectively. Samples are measured in the peak aged condition of 100°C for one hour. It is experiential that both ultimate and yield strength show an increasing trend with the increasing strain rate, and as the strain rate increases, percentages of elongation decreases. Two resulting aspects can be responsible for the positive sensitivity of strain rate to yield strength and flow stress.

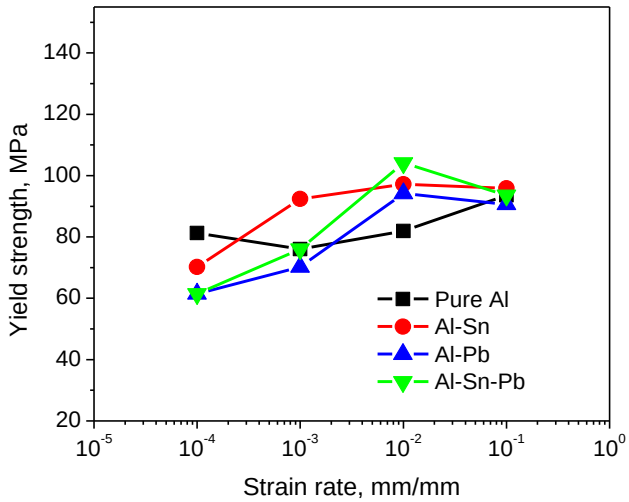

Figure 7: Yield strength of cold-rolled alloys aged at 100°C varies with strain rate.

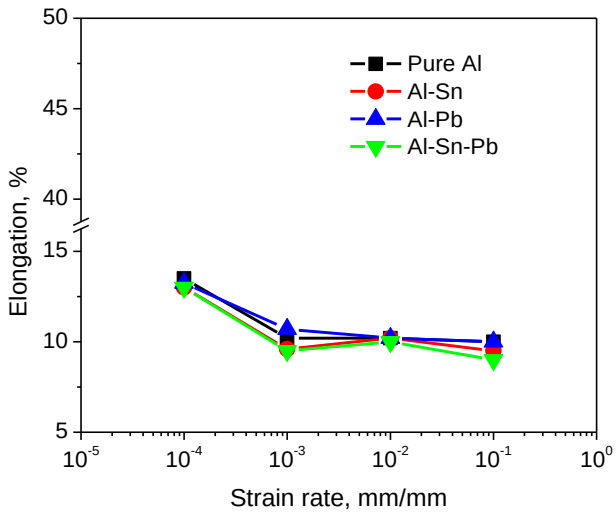

Figure 8: Cold-rolled alloys aged at 100°C show variations in the percentage of elongation with strain rate.

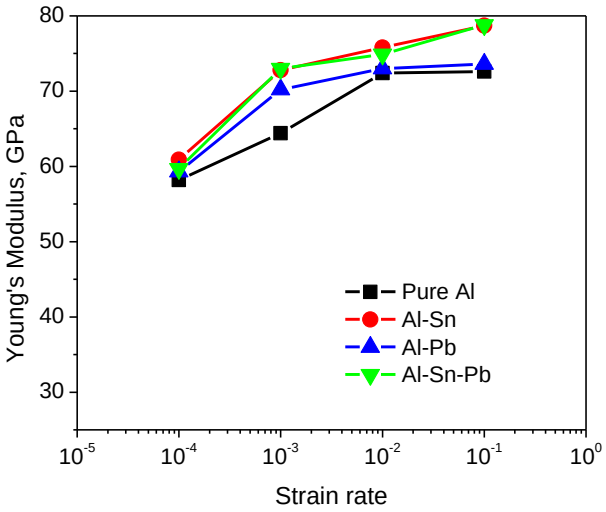

Figure 9: Young's modulus of cold-rolled alloys aged at 100°C varies with strain rate

Higher flow stresses are achieved at higher strain rates since higher strain rates can reduce dislocation annihilation and these strain rates can increase the dislocation speed barrier for active plastic deformation. It is also known that, in comparison to tensile strength, yield strength and flow stress is more reliant on the strain rate. So, the efficacy is higher in case of yield strength (Figures 6 and 7). This observation confirms the earlier finding that mobile of dislocations velocity is linearly proportional to strain rate. During tensile loading, the dislocations movement is strongly prevented by the precipitate present, causing Sn to show higher strength for higher precipitates and lower elongation than pure Al and Al-Pb alloys. Again, at the peak aged condition's maximum precipitation has a significant impact to higher strength as well as lower elongation through inhibiting the dislocation movement, which increases the intensity of Young's modulus with strain rate (Kaiser, 2015; Xu *et al.*, 2017). For solder affected alloys, Sn, Pb added alloys, and then pure Al, the roles of the alloying elements are clearly understood.

3.2 Impact toughness behavior

Impact energy changes of the discussed samples as a function of identical isochronal ageing is shown in Figure 10. A significant difference is observed between them throughout the aging treatment. Pure Al shows an increasing nature of energy absorption with the aging temperature followed by a decreasing trend. This may be evident due to the stress relieving with recovery of 80% severe cold deformed alloys which enhances the energy absorption behaviour of pure Al. Similar fashion with different intensities is observed for Sn added alloy as increasing nature of impact energy around 50°C due to GP zone dissolution, and next one around 150°C for dissolution of Sn into Al. Again, for Pb added alloy energy increase around 50°C

temperature due to GP zone dissolution, and next one around 250°C for dissolution of Pb into Al. Dissolution occurs earlier in case of Sn added alloy because its melting temperature is lower than thar of Pb. This observation can be attributed to the fact that in the course of ageing treatment, the formation of precipitates reduces the impact energy and the dissolution of those phases increases the impact energy. Fine precipitates throughout the ageing process act as primary nucleation, due to which the fracture resistance of the alloy decreases. The impact strength declines relatively high, indicating that the structure of the alloy with added Sn contains more precipitates. Then higher aging temperatures allow recrystallization as a new set of grains like cast alloys as well as at this overaged condition alloys lose their brittleness as coarse particles reduce pinning effects. The solder affected alloy follows both the elements Sn and Pb effect (Khan *et al.*, 2023).

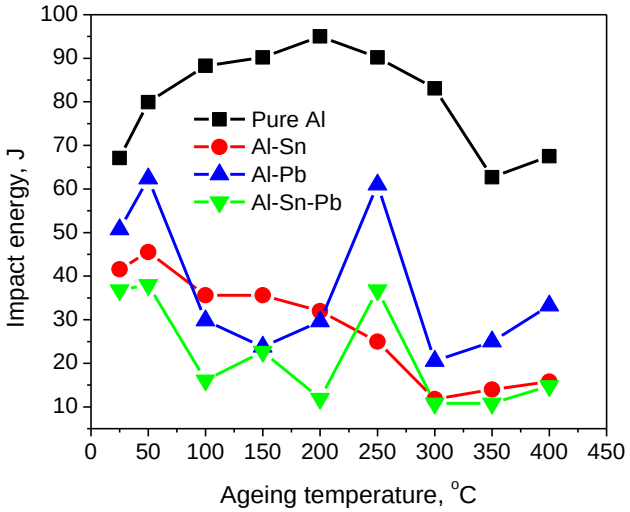

Figure 10: Impact characteristics of 80% cold rolled alloys affected by aging.

3.3 Optical micrographs

Optical images of investigated Al, Al-Sn, Al-Pb and Al-Sn-Pb alloys aged at 100°C for one hour are shown in Figure 11. Ageing at this temperature and time duration normally does not alter the grain orientation of Al-alloys. Stress may be relieved as well as developed various precipitates in the alloy (Kaiser, 2020a; Rokon *et al.*, 2023). These phenomena also conform to the outcome of strengthening qualities. The microstructures exhibit regularly elongated grains in the rolling direction as the alloys are cold rolled by 80%. But the severe deformation makes the crystal grains indistinct and difficult to distinguish. Thus, pure Al consists of the solid phases of α-Al and various intermettalics in the microstructure which formed by the trace impurities (Figure 11a). The tin added alloy microstructure is fully composed of primary aluminum, β-tin along with a variety of impurity intermettalics (Figure 11b). Since its BCC crystal structure is different from the FCC of Al, it tends to distribute at grain boundaries, which makes the grain boundaries denser. This is one

of the cases of improvement the higher hardness of the Sn added alloy. Likewise, lead containing alloy shows primary aluminium, α-lead and impurities distributed in the microstructure (Figure 11c). But the grain boundaries are not very thick because both Pb and Al alloys have the FCC crystal structure. So, the experimental hardness of Pb shows lower compare to Sn added alloy. The solder affected alloy replicates the addition of together elements on the microstructure as well as the microhardness (Figure 11d) (Noskova *et al.*, 2008).

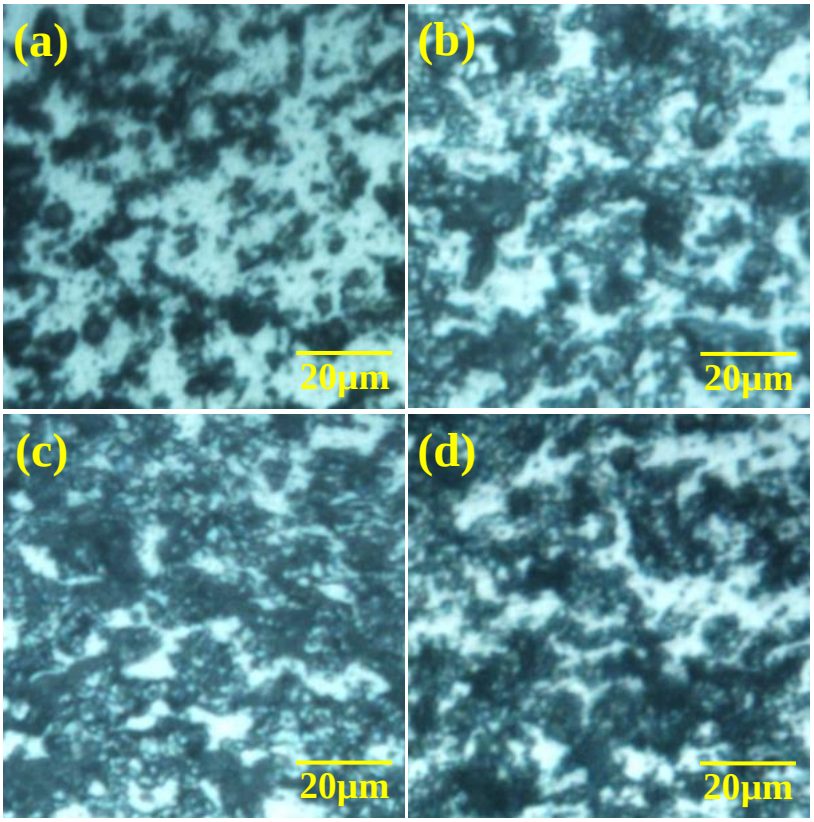

Figure 11: Optical micrograph (a) Al, (b) Al-Sn, (c) Al-Pb and (d) Al-Sn-Pb alloys.

3.4 SEM observation

In Figure 12, it is presented the fracture mode of the above four investigated samples when tensile tested at a strain rate of 10^{-3}/s and analysis by SEM. Clear differences are observed between images of the fracture surfaces. This is a simple fracture similar to the mixed intergranular and trans-granular ductile fracture (Figure 12a) for pure Al. As it consists of various trace impurities, trace second-phase particles are formed as distributions along grains and grain boundaries which promote microcracks (Kaiser, 2020b). The fracture surfaces also contain several dimples that support the scenario of the ductile fracture. In case of Sn doping alloy dimples along with some smooth, flat areas intersperse with bright ridges of foreign particles

(Figure 12b). Due to the different BCC structure from FCC Al, Sn phases tend to distribute along the grain boundaries. This results in thickening of grain boundaries where fracture initiates. So, the number of dimples is high and small in sizes. Alike an FCC crystal structure of Al and Pb and Pb does not form various intermettalics, the fracture mode is somewhat similar to that of pure Al (Figure 12c). Pb phases added some path to fracture (Han *et al.*, 2023; Kaiser, 2020b). Al/Sn system has higher strengthening ability than that of the Al/Pb system due to the different solid solubility, which is consistent with the nature of fracture. As can be seen from Figure 12d, the fracture surface of the solder-affected alloy fully obeys the combined impact nature of Sn and Pb elements.

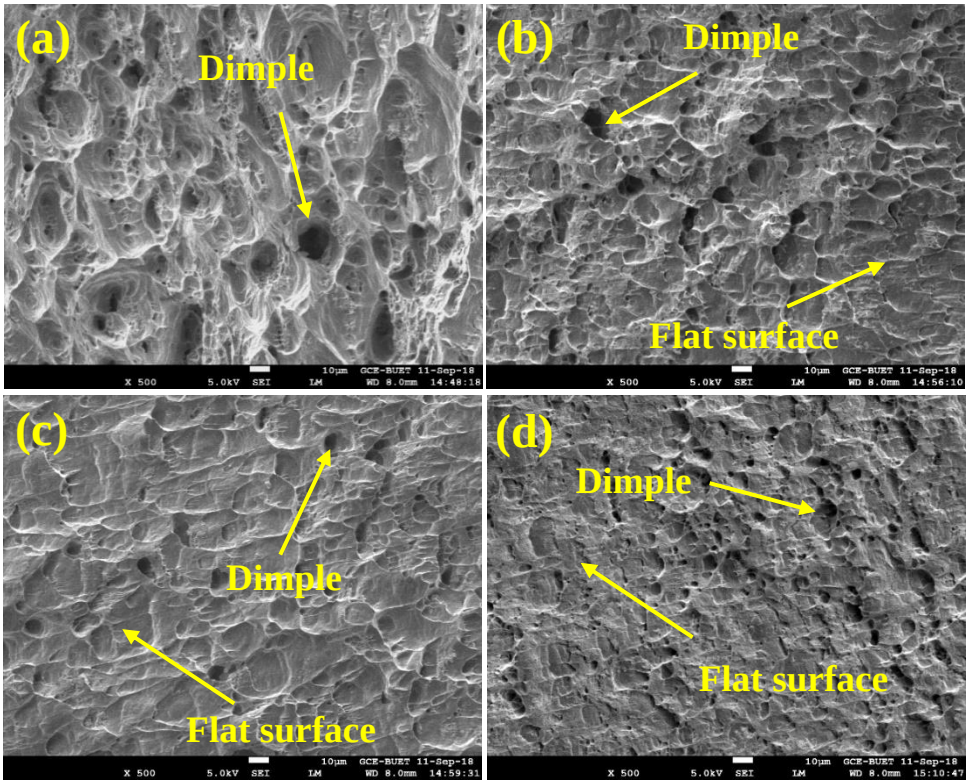

Figure 12: SEM fracture surfaces (a) Al, (b) Al-Sn, (c) Al-Pb and (d) Al-Sn-Pb alloys.

4. Conclusion

Examining the outcomes of impact and tensile tests conducted on pure aluminum, Al-Sn alloy, Al-Pb alloy, and Sn/Pb-solder affected Al reveal that

Due to solute solution strengthening minor Sn-Pb solder has a vast impact at the mechanical properties of commercially pure aluminium. Sn exhibits higher strength of the alloy than Pb due to its BCC crystal structure which is different from FCC Al crystal structure like Pb.

Both Sn and Pb do not form any intermetallic with Al, but during ageing those elements create different intermetallic with cast impurities and improve the strength specially Sn. Consequently, the elongation decreases while the tensile strength increases at higher strain rates.

Impact energy also follows percentages elongation as it decreases in the peak aging state and increases in the overaged state. At higher ageing temperature extremely fall alloys' strength due to over ageing effects where produces a new set of grains like cast alloys.

For alloys with small additions, thicker grain boundaries are seen and the microstructures are made up of grains that are elongated in the rolling direction.

Doping Sn shows higher dimples along with some smooth, flat areas in microstructure as fracture through the grain boundary, but mixed fracture is observed for Pb added alloy and the solder affected alloy shows both effects.

Electrical and thermal conductivity are major thrust areas that need to be explored for further study to determine the manufacturing feasibility of these low-response age-hardenable wrought alloys.

Acknowledgment

It is acknowledged that the Miyan Research Institute provided financial support for the project work. The author would like to express his appreciation to the Director of Administration, for all of the helpful support and encouragement she has made available in advancing research activities at IUBAT, Dhaka.

Conflict of interest

The author states that there are no potential conflicts of interest with regard to the publishing of this work. Furthermore, he possesses direct experience with all ethical concerns, including redundancy, plagiarism, informed consent, misconduct, data fabrication or falsification, and duplicate publishing or submission.

References

Ard, P. M., Uthaisangsuk,V., Tosangthum,N., Sheppard, P., Wila, P., & Tongsri, R. (2015). Fe-Sn Intermetallics Synthesized via Mechanical Alloying-Sintering and Mechanical Alloying-Thermal Spraying. *Key Engineering Materials*, 659, 329-334. https://doi.org/10.4028/www.scientific.net/KEM.659.329

ASM Handbook Committee. (1990). Properties and Selection: Nonferrous Alloys and Special-Purpose Materials, *ASM International*, Volume 2, Materials Park, Ohio, USA.

Bhat, J., Pinto, R., & Satyanarayan. (2021). A review on effect of alloying elements and heat treatment on properties of Al-Sn alloy. *Materials Today: Proceedings*, 35(3), 340-343. https://doi.org/10.1016/j.matpr.2020.01.617

Davis, J. R. (2001). Alloying: Understanding the Basics. *ASM International*, Materials Park, Ohio, USA.

Guan, Q., Hang, C., Li, S., Yu, D., Ding, Y., Wang, X., & Tian, Y. (2023). Research progress on the solder joint reliability of electronics using in deep space exploration. *Chinese Journal of Mechanical Engineering*, 36(22), 1-13. https://doi.org/10.1186/s10033-023-00834-4

Han, S., Lezaack, M. B., Pyka, G., Netto, N., Simar, A., Wahab, M. A., & Hannard, F. (2023). On the Competition between Intergranular and Transgranular Failure within 7xxx Al Alloys with Tailored Microstructures. *Materials*, 16(3770), 1-18. https://doi.org/10.3390/ma16103770

Kaiser, M. S. (2021). Effect of trace impurities on the thermoelectric properties of commercially pure aluminium. *Materials Physics and Mechanics*, 47(4), 582-591. https://doi.org/10.18149/MPM.4742021_5

Kaiser, M. S. (2020a). Fractional recrystallization behavior of impurity-doped commercially pure aluminum. *Journal of Energy, Mechanical, Material, and Manufacturing Engineering, 5(2)*, 37-46. https://doi.org/10.22219/jemmme.v5i2.11675

Kaiser, M. S. (2020b). Trace impurity effect on the precipitation behaviuor of commercially pure aluminium through repeated melting. *European Journal of Materials Science and Engineering*, 5(1), 37-48. https://doi.org/10.36868/ejmse.2020.05.01.037

Kaiser, M. S. (2015). Tensile and Fracture Behavior of Wrought Al-6Mg Alloy with Ternary Scandium and Quaternary Zirconium and Titanium Addition. *International Journal of Materials Science and Engineering*, 3(2), 147-158.

Khan, A. A., Hossain, A. K., & Kaiser, M. S. (2023). Role of Si at a lower level on the mechanical properties of Al-based automotive alloy. *Journal of Mining and Metallurgy, Section B: Metallurgy*, 59(1), 149-156. https://doi.org/10.2298/JMMB230131013K

McAlister, A. J. (1984). The Al-Pb (Aluminum-Lead) system. *Bulletin of Alloy Phase Diagrams*, 5, 69-73. https://doi.org/10.1007/BF02868728

McAlister, A. J., & Kahan, D. J. (1983). The Al-Sn (Aluminum-Tin) System. *Bulletin of Alloy Phase Diagrams*, 4, 410-414. https://doi.org/10.1007/BF02868095

Nagy, E., Kristaly, F., Gyenes, A., & Gacsi, Z. (2015). Investigation of intermetallic compounds in Sn-Cu-Ni lead-free solders. *Archives of Metallurgy and Materials*, 60(2), 1511-1515. https://doi.org/10.1515/amm-2015-0163

Noskova, N. I., Korshunov, L. G., & Korznikov, A. V. (2008). Microstructure and tribological properties of Al-Sn, Al-Sn-Pb, and Sn-Sb-Cu alloys subjected to severe plastic deformation. *Metal Science and Heat Treatment*, 50, 593-599. https://doi.org/10.1007/s11041-009-9104-1

Paraskevas, D., Ingarao, G., Deng, Y., Duflou, J. R., Pontikes, Y., & Blanpain, B. (2019). Evaluating the material resource efficiency of secondary aluminium production: A Monte Carlo-based decision-support tool. *Journal of Cleaner Production*, 215, 488-496. https://doi.org/10.1016/j.jclepro.2019.01.097

Prabhu, T. R. (2017). Effects of ageing time on the mechanical and conductivity properties for various round bar diameters of AA 2219 Al alloy, *Engineering Science and Technology, an International Journal*, 20(1), 133-142. https://doi.org/10.1016/j.jestch.2016.06.003.

Rokon, N., Haque, M. S., & Kaiser, M. S. (2023). On the mechanical behaviour of thermally affected non-heat-treatable aluminium alloys, *Journal of Chemical Technology and Metallurgy*, 58(6), 1153-1162. https://doi.org/10.59957/jctm.v58i6.156

Shoummo, M. R., Khan, A. A., & Kaiser, M. S. (2022). True stress-strain behavior of Al-based cast automotive alloy under different ageing conditions and the effect of trace Zr. *Journal of Mechanical Engineering Science and Technology*, 6(2), 95-106. https://doi.org/10.17977/um016v6i22022p095

Sivasankaran, S. (2017). Aluminium alloys-recent trends in processing, Characterization, Mechanical Behavior and Applications, *IntechOpen*, London, UK.

Stamenkovic, U., Ivanov, S., Markovic, I., Balanovic, L., & Gorgievski, M. (2019). The effect of precipitation of metastable phases on the thermophysical and mechanical properties of the EN AW-6082 alloy. *Revista de Metalurgia*, 55(4), 1-7. https://doi.org/10.3989/revmetalm.156

Tehrani, M. (2021). Advanced Electrical Conductors: An Overview and Prospects of Metal Nanocomposite and Nanocarbon Based Conductors. *Physica Status Solidi (A) Applications and Materials*, 218(8), 1-17. https://doi.org/10.1002/pssa.202000704

Woodcraft, A. L. (2005) Recommended values for the thermal conductivity of aluminium of different purities in the cryogenic to room temperature range, and a comparison with copper. *Cryogenics*, 45(9), 626-636. https://doi.org/10.1016/j.cryogenics.2005.06.008

Xu, P., Luo, H., Li, S., Lv, Y., Tang, J., & Ma, Y. (2017). Enhancing the ductility in the age-hardened aluminum alloy using a gradient nanostructured structure. *Materials Science and Engineering: A*, 682, 704-713. https://doi.org/10.1016/j.msea.2016.11.090